Electronic Supplementary Material (ESI) for Soft Matter.

Supporting Information for

Proving and interpreting the spontaneous formation of bulk nanobubbles in aqueous organic solvent solutions: effects of solvent type and content

Ananda J. Jadhav, Mostafa Barigou✉

School of Chemical Engineering, University of Birmingham, Edgbaston, Birmingham B15 2TT, United Kingdom

Nanoparticle tracking analysis

Measurements were conducted at 25 ˚C using a blue laser light source (70 mW, λ = 405 nm). The sample was introduced using a syringe pump (flowrate set to 100 in arbitrary units). NTA is based on a laser-illuminated microscopic technique and the Brownian motion of BNBs in solution is detected and recorded by a scientific CMOS camera. A video of the scattered light from the bubble in a flow field was recorded in triplicates, each recording lasting 60 s at a camera level of 13−16. Subsequently, a particle tracking image analysis program (i.e., the NTA software version 3.2) determines the size distribution by tracking the visualized bubbles simultaneously but separately. The analysis parameters used were the threshold set within 5 to 10 to avoid noise, and the gain set to 512. Prior to NTA measurements, the visualisation cell was first rinsed with pure water and dried with dry Nitrogen gas.

Zeta potential measurements

Zeta potential is the potential difference between the dispersion medium and the stationary layer of fluid attached to the dispersed colloidal particle. Zeta potential cannot be measured directly, but it can be derived using a theoretical model and an experimentally determined electrophoretic mobility of charged entities under an applied electric field. The electrophoretic mobility, μ_e, is defined as

$$\mu_e = \frac{u}{E} \tag{1}$$

where u is the drift velocity of the dispersed particle and E is the strength of the applied electric field.

Thus, the zeta potential, ζ, can be calculated from

$$\mu_e = \frac{2\varepsilon_r \varepsilon_0 \zeta f(\kappa a)}{3\eta} \tag{2}$$

where ε_r, ε_0, η, and $f(\kappa\alpha)$ are the relative permittivity or dielectric constant of the dispersion medium, the permittivity of vacuum, the dynamic viscosity of the dispersion medium at the experimental temperature, and Henry's function, respectively, which describes the electrophoretic mobility of a spherical colloidal particle in the limit of low surface potentials.

Solvent separation from BNB suspensions

The separation of solvent from BNB suspension was carried out at 50 ˚C in a rotary vacuum evaporator (RV 8 V-C, IKA, UK) using a vacuum (boiling) pressure of 594 mbar for methanol-water; 291 mbar for ethanol-water; 224 mbar for propanol-water; 806 mbar for acetone-water; 120 mbar for DMSO-water; and 120 mbar for formamide-water. The rotary evaporator experiments are schematically illustrated in Figure S1.

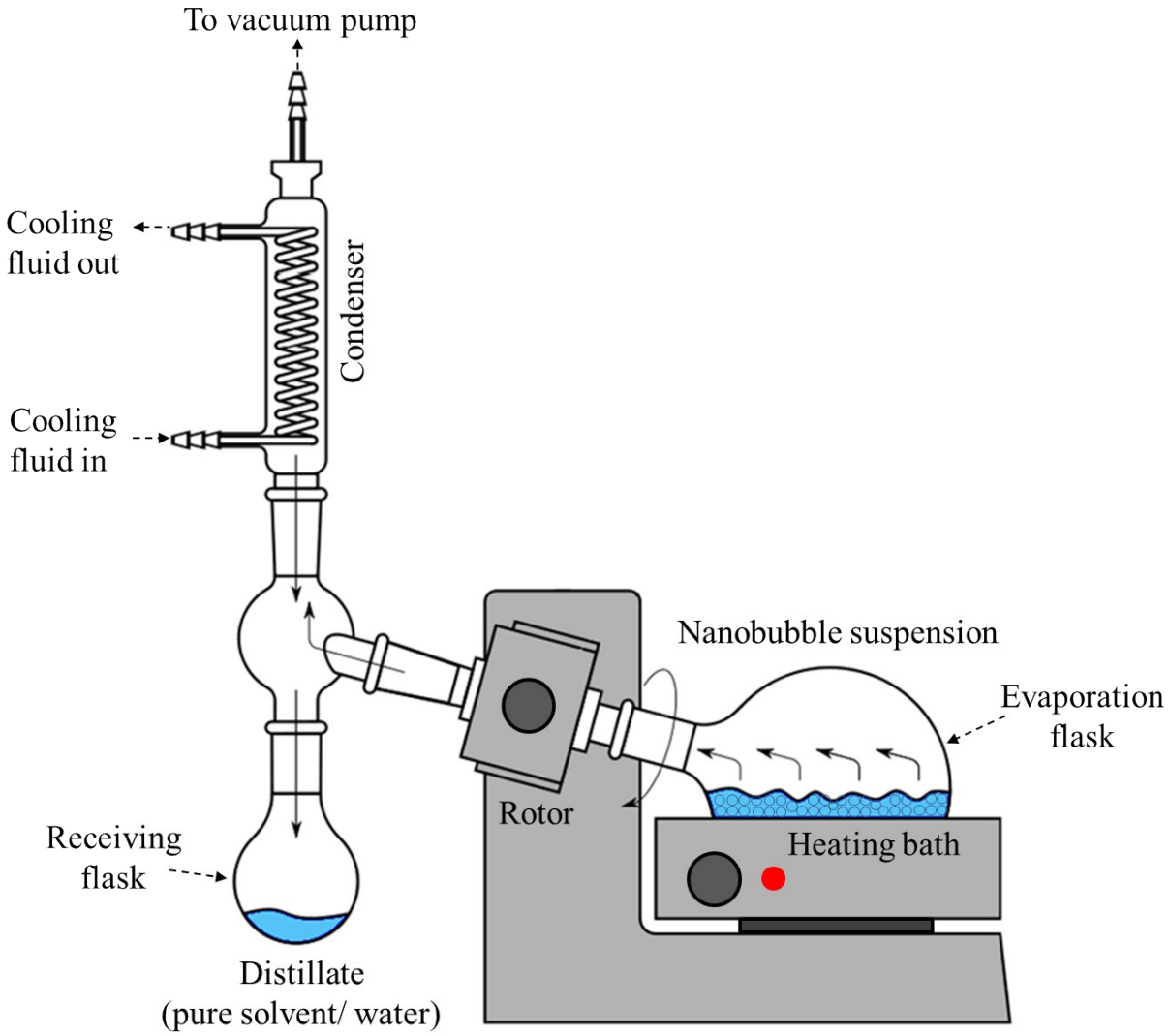

Figure S1. Schematic of vacuum rotary evaporator experiments.

FT-IR analysis

FT-IR is a non-destructive, quantitative, and quick method for identifying a wide range of chemical constituents and elucidating compound structures in various forms in real-world samples according to the vibrational modes of their molecular functional groups. FT-IR

spectroscopic measurements were used here to investigate the purity of bulk nanobubble suspensions produced in water-solvent mixtures. Spectroscopic measurements were performed on a Tensor 27 instrument (Bruker, Germany) coupled with an ATR accessory. The scanned spectral range was from 400−4000 cm^{-1}, with a resolution of 2 cm^{-1} and a wavenumber accuracy of 0.01 cm^{-1}.

GC-MS analysis

GC-MS analysis of water and BNB suspensions was performed with an Agilent 7890A gas chromatograph (Agilent Technology, UK) equipped with ZB-WAX column (30 m × ϕ 0.25 mm, thickness 0.25 μm, Phenomenex, UK) coupled to a GCT Premier mass spectrometer (Waters, UK) operated in electron ionization (EI^+) mode. Helium was used as a carrier and make-up gas passed through the column at a constant flowrate of 1.0 $mL.min^{-1}$. The injection volume was 1 μL, which was used with a split ratio of 1:10. The column temperature programme was as follows: temperature was held at 50 ˚C for 2 min, increased to 250 ˚C at 5 ˚$C.min^{-1}$ and then held at 250 ˚C for 18 min. The GC-MS operating parameters are summarized in Table S1.

Table S1. GC-MS operating parameters.

Gas chromatography	
Instrument	7809A (Agilent)
Column	ZB−WAX 30 m × ϕ 0.25 mm, 0.25 μm (Phenomenex, UK)
Injection method	Split (1:10)
Injection volume	1 μL
Carrier gas	Helium
Flow rate	1 $mL.min^{-1}$
Injection temperature	250 ˚C
Oven temperature program	50 ˚C (2 min) → 5 ˚C/min → 250 ˚C (18 min)
Transfer line temperature	250 ˚C
Mass spectrometry	
Instrument	GCT Premier (Waters, UK)
Mode	Selected-ion monitoring
Ion source temperature	250 ˚C
Ionization mode	Electron impact (EI^+)
Electron energy	70 eV
Trap current	100 μA
Emission current	179 μA

ICP-MS analysis

A NexION 300X ICP-MS spectrometer (Perkin-Elmer, UK) equipped with a cyclonic spray chamber and a SeaSpray concentric nebulizer was used to analyse pure water and BNB suspensions for the presence of any trace metal particles. The ICP-MS operating parameters are summarised in Table S2. In order to quantify the analytical results of ICP-MS, the internal and external standard additions modes were used. All standards were prepared in a 2% aqueous solution of HNO_3. Single element stock solutions (Sigma Aldrich, UK) of 32 metals, namely Na, Mg, Al, Si, P, K, Ca, Ti, V, Cr, Mn, Fe, Co, Ni, Cu, Zn, Rb, Sr, Zr, Ru, Rh, Pd, Ag, Cd, Sn, Sb, Te, Hf, Ir, Pt, Au, and Hg at a 1000 ppm concentration were used to prepare the standards for external calibration. The calibration curve and corresponding correlation coefficient ($R^2 > 0.99$) for each metal element used are presented in the Figures S2−S4. Indium at 1 ppm was employed as internal standard. Pure water and BNB suspensions were acidified using 2 % HNO_3 prior to ICP-MS sampling. Samples were supplied to the nebulizer in continuous mode with the spectrometer peristaltic pump using flared end PVC-based tubing of 0.19 mm internal diameter.

Table S2. ICP-MS operating parameters.

Parameter	Value
RF applied power (kW)	1.6 kW
Auxiliary gas flow rate (Argon)	1.2 $L.min^{-1}$
Plasma gas flow (Argon)	18 $L.min^{-1}$
Nebulizer gas flow (Argon)	0.95 $L.min^{-1}$
Sample flow rate	0.3 $mL.min^{-1}$
KED Gas Flow (Helium)	4 $mL.min^{-1}$
Nebulizer type	Sea Spray concentric
Interface cone material	Nickel
Analog stage voltage	-1675
Pulse stage voltage	1050 V
Discriminator threshold	12 mV
Deflector voltage	- 10 V
Quadrupole rod offset	- 12 V
Cell entrance voltage	- 9 V
Cell exit voltage	- 20 V
Cell rod offset	- 15 V
Axial field voltage	475 V

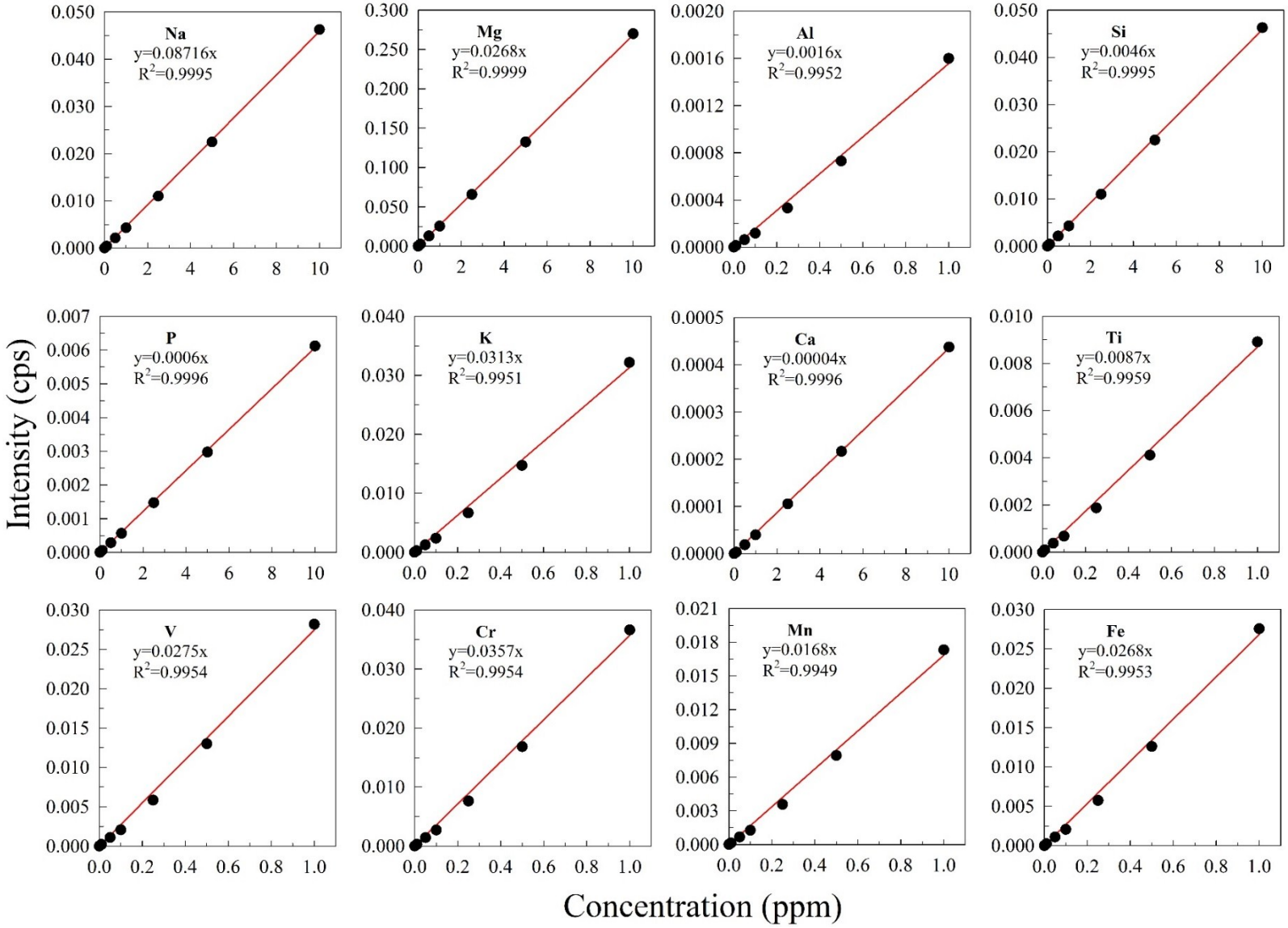

Figure S2. Calibration curves for individual elements (Na, Mg, Al, Si, P, K, Ca, Ti, V, Cr, Mn, Fe) measured by ICP-MS with solution-based calibration (standard additions mode).

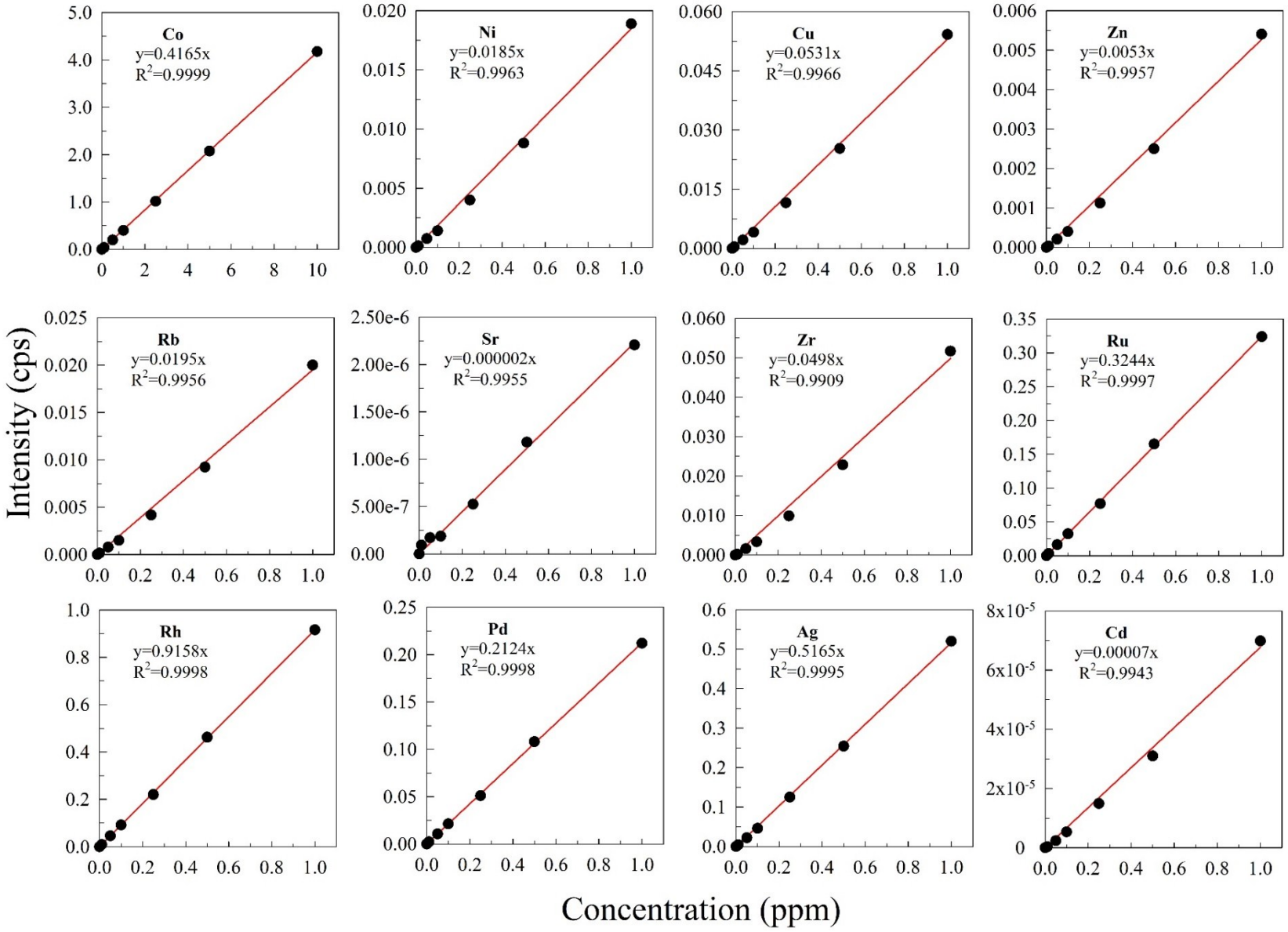

Figure S3. Calibration curves for individual elements (Co, Ni, Cu, Zn, Rb, Sr, Zr, Ru, Rh, Pd, Ag, Cd) measured by ICP-MS with solution-based calibration (standard additions mode).

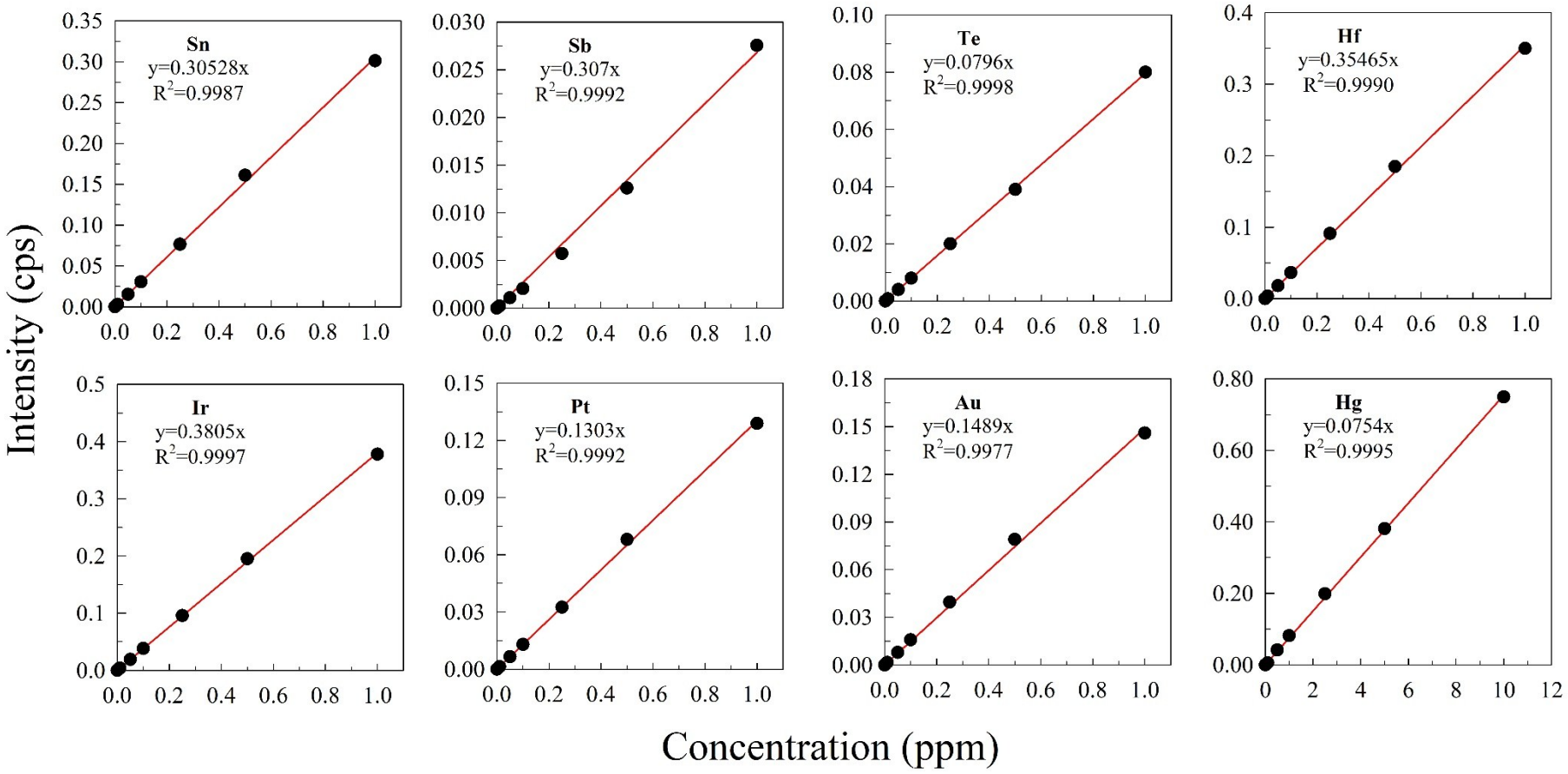

Figure S4. Calibration curves for individual elements (Sn, Sb, Te, Hf, Ir, Pt, Au, Hg) measured by ICP-MS with solution-based calibration (standard additions mode).

Table S3. Concentration (in ppm) of metal elements in pure water and in BNB suspensions measured using ICP-MS.

Element	System						
	Pure water	Methanol–water	Ethanol–water	Propanol–water	Acetone–water	DMSO–water	Formamide–water
Na	0.00172133	0.00444038	0.00125743	0.00053166	0.00003241	0.00189523	0.00346274
Mg	0.00340853	0.09470772	0.08829229	0.05138736	0.20154953	0.02422444	0.02419850
Al	0.00149442	0.00370117	0.00384816	0.00373197	0.01034759	0.00027070	0.02636626
Si	0.00661920	0.00123500	0.00189750	0.00012400	0.00124600	0.00178133	0.00025640
P	0.00018715	0.07952907	0.07844375	0.06722927	0.09663056	0.00589521	0.18847636
K	0.00083072	0.00007525	0.00066579	0.00094059	0.00011608	0.00011355	0.00024982
Ca	0.00195125	0.01564467	0.01895287	0.00460719	0.00050294	0.64505524	0.01110064
Ti	0.00002289	0.00152472	0.00033280	0.00058514	0.00506937	0.00025895	0.00081620
V	0.00013583	0.00009470	0.00008020	0.00012915	0.00002945	0.00013054	0.00002281
Cr	0.00001050	0.00575419	0.00556784	0.00483426	0.00478125	0.00003040	0.00216302
Mn	0.00004247	0.00002125	0.00013241	0.00013807	0.00009924	0.00014995	0.00001281
Fe	0.00465229	0.00447190	0.00014199	0.00022143	0.00051562	0.00000279	0.00351205
Co	0.00040516	0.00009572	0.00007699	0.00029002	0.00038570	0.01747969	0.00006946
Ni	0.00011337	0.00018425	0.00007115	0.00008747	0.00006685	0.00012769	0.00051004
Cu	0.00000952	0.00019110	0.00001537	0.00001730	0.00015227	0.00012302	0.00012029
Zn	0.00020725	0.01737608	0.00061665	0.00080742	0.00116325	0.00003025	0.00157693
Rb	0.00014648	0.00015334	0.00015974	0.00015974	0.00015462	0.00015391	0.00014814
Sr	0.00016930	0.00247027	0.00276589	0.00309927	0.00365305	0.00013242	0.00041762
Zr	0.00016458	0.00019320	0.00019673	0.00019645	0.00016686	0.00019167	0.00015318
Ru	0.00000031	0.00005102	0.00000936	0.00000218	0.00060489	0.00000042	0.00000119
Rh	0.00006193	0.00003113	0.00000817	0.00000243	0.00022442	0.00004410	0.00043564
Pd	0.00000009	0.00002945	0.00000824	0.00000259	0.00030689	0.00000134	0.00004948
Ag	0.00006130	0.00021071	0.00019958	0.00017864	0.00000659	0.00026172	0.00001560
Cd	0.00024978	0.03780023	0.00243503	0.00153898	0.19729668	0.00022163	0.00003102
Sn	0.00003272	0.00004958	0.00006099	0.00004100	0.00025320	0.00000170	0.00003449
Sb	0.00000430	0.00002551	0.00001294	0.00000973	0.00017189	0.00000041	0.00002155
Te	0.00000579	0.00000960	0.00000205	0.00000432	0.00020947	0.00000786	0.00000026
Hf	0.00000060	0.00000043	0.00000002	0.00000013	0.00001112	0.00000003	0.00000873
Ir	0.00000210	0.00000721	0.00000157	0.00000335	0.00005958	0.00000046	0.00078019
Pt	0.00000720	0.00002139	0.00001218	0.00000911	0.00005361	0.00000252	0.00008411
Au	0.00000184	0.00000433	0.00000126	0.00000157	0.00002872	0.00000015	0.00002785
Hg	0.03703924	0.01796302	0.01097952	0.00848094	0.02731036	0.08859078	0.03734123